agriculture

MDPI

Article

Field Validation of the DNDC-Rice Model for Crop Yield, Nitrous Oxide Emissions and Carbon Sequestration in a Soybean System with Rye Cover Crop Management

Qiliang Huang [1], Nobuko Katayanagi [2,*], Masakazu Komatsuzaki [3] and Tamon Fumoto [2]

[1] United Graduate School of Agriculture Science, Tokyo University of Agriculture and Technology, 3-5-8 Saiwai-cho, Fuchu, Tokyo 183-8509, Japan
[2] Institute for Agro-Environmental Sciences, National Agriculture and Food Research Organization, 3-1-3 Kannondai, Tsukuba, Ibaraki 305-8604, Japan; fumoto.tamon877@naro.go.jp
[3] College of Agriculture, Ibaraki University, 3-21-1 Ami, Ibaraki 300-0393, Japan; masakazu.komatsuzaki.fsc@vc.ibaraki.ac.jp
* Correspondence: katayanagi.nobuko463@naro.go.jp; Tel.: +81-298388797

Abstract

The DNDC-Rice model effectively simulates yield and greenhouse gas emissions within a paddy system, while its performance under upland conditions remains unclear. Using data from a long-term cover crop experiment (fallow [FA] vs. rye [RY]) in a soybean field, this study validated the DNDC-Rice model's performance in simulating soil dynamics, crop growth, and C-N cycling processes in upland systems through various indicators, including soil temperature, water-filled pore space (WFPS), soybean biomass and yield, CO_2 and N_2O fluxes, and soil organic carbon (SOC). Based on simulated results, the underestimation of cumulative N_2O flux (25.6% in FA and 5.1% in RY) was attributed to both underestimated WFPS and the algorithm's limitations in simulating N_2O emission pulses. Overestimated soybean growth increased respiration, leading to the overestimation of CO_2 flux. Although the model captured trends in SOC stock, the simulated annual values differed from observations (−9.9% to +10.1%), potentially due to sampling errors. These findings indicate that the DNDC-Rice model requires improvements in its N cycling algorithm and crop growth sub-models to improve predictions for upland systems. This study provides validation evidence for applying DNDC-Rice to upland systems and offers direction for improving model simulation in paddy-upland rotation systems, thereby enhancing its applicability in such contexts.

Keywords: DNDC-Rice; greenhouse gas; soil organic carbon; cover crop

check for updates

Academic Editor: Lijun Liu

Received: 22 May 2025
Revised: 4 July 2025
Accepted: 7 July 2025
Published: 15 July 2025

Citation: Huang, Q.; Katayanagi, N.; Komatsuzaki, M.; Fumoto, T. Field Validation of the DNDC-Rice Model for Crop Yield, Nitrous Oxide Emissions and Carbon Sequestration in a Soybean System with Rye Cover Crop Management. *Agriculture* **2025**, *15*, 1525. https://doi.org/10.3390/agriculture15141525

Copyright: © 2025 by the authors. Licensee MDPI, Basel, Switzerland. This article is an open access article distributed under the terms and conditions of the Creative Commons Attribution (CC BY) license (https://creativecommons.org/licenses/by/4.0/).

1. Introduction

Agricultural production is a significant source of greenhouse gas (GHG) emissions, which are key drivers of climate change [1]. Extreme climate events, in turn, reduce agricultural yields, thereby threatening global food security [2]. Agricultural soils can function as either sources or sinks of GHGs, depending on various conditions [3]. Implementing effective agricultural management practices to reduce GHG emissions and enhance carbon (C) sequestration is a crucial strategy for mitigating climate change at the agricultural level.

In recent years, conservation agricultural management practices have rapidly spread due to their ability to enhance ecosystem services and promote sustainable agricultural development [4]. Cover crop management, a typical and historic conservation agriculture

method, has undergone massive studies that have confirmed its positive effect on mitigating soil erosion [5], improving soil structure and water-stable aggregates [6,7], enhancing soil fertility [8], and reducing weed infestation [9,10]. For example, a cover crop experiment conducted in Japan demonstrated that a rye cover crop significantly improved soil health within a soybean cropping system [11]. However, the impact of cover crops on GHG emissions and soil C sequestration remains contentious. Some studies have reported that cover crops can reduce nitrous oxide (N_2O) emissions by scavenging excess NO_3-N in the soil [12,13]. The biomass remaining after cover crop termination serves as a C source, contributing to increased soil organic carbon (SOC) stocks [14,15]. However, the release of organic C and nitrogen (N) during the decomposition of cover crop residues may also result in elevated N_2O emissions [16,17]. These increased N_2O emissions, in turn, could potentially offset the climate change mitigation benefits associated with the enhanced SOC stocks [18,19]. The potential of cover crops to mitigate climate change varies based on factors such as site characteristics, agronomic practices, and cover crop species [18,20]. Consequently, evaluating the effect of cover crops on climate change requires incorporating context-specific considerations.

Although field experiments can provide direct observations of GHG emissions and SOC stock at a specific point in time, they are difficult to use for continuous monitoring of intermediate processes, such as the C–N–water–crop balances [21]. Additionally, field experiments are resource-intensive and time-consuming due to the necessity of conducting extensive repeated measurements [22]. A well-calibrated model has the capacity to simulate the physical, chemical, and microbiological processes in soil using mathematical principles and computational power to calculate soil GHG emissions [23]. Simulation models are diverse, varying in complexity from simple empirical estimates based on statistical analysis to complex process-based biogeochemical models [23,24]. The DeNitrification-Decomposition (DNDC) model, a process-based model, focuses on the C and N biogeochemistry in an agro-ecosystem [25]. By integrating classical physics, chemistry, and biology laws, the model is capable of parameterizing specific geochemical or biochemical processes, such as simulating and quantifying the GHG emissions, as well as C and N dynamics in soil [26]. Currently, the DNDC model is widely adopted to estimate and compare the GHG mitigation potential across diverse agricultural management scenarios at regional and national scales [27,28]. Moreover, the DNDC model has been modified numerous times and integrated with various sub-models to produce different versions to meet the specific needs of different regions, agronomic management, and crops. For instance, DNDC-Rice is a revised version specifically designed for rice cultivation [29]. The DNDC-Rice model significantly enhances the ability to estimate greenhouse gas emissions from paddy fields and has been validated using GHG data from paddy fields across Asia, including Japan [30], India [31], and Thailand [32]. It demonstrates high accuracy and performance in simulating and predicting greenhouse gas emissions from paddy fields under different irrigation management scenarios [31].

In rice production systems, alongside the prevalent practice of continuous rice monoculture, the rotation of paddy with upland crops is also commonly employed [33]. Numerous studies have reported that the DNDC-Rice model is a powerful tool for accurately estimating soil GHG emissions in the continuous rice monoculture system [28,34]. In rice systems with paddy-upland rotation, it is impractical to use different versions of the DNDC model to simulate and predict the paddy and upland periods separately. Additionally, DNDC-Rice has incorporated substantial modifications for rice cultivation, while maintaining nearly identical crop models for non-rice crops as the original DNDC version. Consequently, simulations for non-rice crops can be performed similarly to the original DNDC framework. Furthermore, the model includes improvements in shared biogeochem-

ical processes (e.g., denitrification) that occur in both upland and paddy systems, which are expected to enhance its performance compared to the original DNDC framework. However, field validation of the DNDC-Rice model for N_2O emissions in upland cropping systems remains limited. This gap highlights the novelty and necessity of validating DNDC-Rice under upland management practices. Furthermore, previous studies have primarily focused on estimating GHG emissions, while field validations concerning the dynamics of C sequestration are still scarce.

Thus, we conducted a field validation of the DNDC-Rice using data from a long-term soybean-cover crop cropping system, with particular focus on evaluating the performance of sub-models related to C dynamics, N dynamics, and crop growth. This study aims to address the gap in the validation of the DNDC-Rice model for upland systems, thereby advancing its application in simulating paddy-upland rotation systems. Specifically, the objectives of this study were to: (1) evaluate the performance of the DNDC-Rice model in simulating N_2O emissions and SOC stock dynamics in an upland cropping system with a cover crop; and (2) discuss the strategies to improve the accuracy of the predictions.

2. Materials and Methods

2.1. The DNDC-Rice Model

The DNDC model, developed by Li et al. at the University of New Hampshire, Durham, NH, USA, is a process-based model to simulate greenhouse gases, such as N_2O, carbon dioxide (CO_2), and methane (CH_4), from agricultural ecosystems [26] by focusing on the C and N biogeochemistry in agro-ecosystem [25]. The DNDC model is organized into two primary components, which together consist of six sub-models. The first component includes sub-models for simulating soil microclimate, plant growth, and organic matter decomposition. These sub-models operate based on key environmental drivers such as climate conditions, soil properties, vegetation type, and land management, and they predict variables such as soil temperature, moisture content, pH, and substrate concentrations. The second component contains sub-models that represent nitrogen cycling and fermentation processes, specifically denitrification, nitrification, and methane dynamics. These sub-models estimate the fluxes of trace gases, including CO_2, CH_4, NH_3, NO, N_2O, and N_2 by modeling soil microbial and chemical transformations [26,35,36].

DNDC-Rice version 2021R2 is a revised version of the DNDC model, developed based on DNDC version 8.2L, primarily designed to simulate CH_4 emission from rice paddies [29,30]. The revised model quantifies the production of electron donors [H_2 and dissolved organic carbon (DOC)] by decomposition and rice root exudation, and simulates CH_4 production and other reductive reactions based on the availability of electron donors and acceptors (NO_3^-, Mn^{4+}, Fe^{3+}, and SO_4^{2-}) under anaerobic soil processes. Rice growth process and CH_4 emission through rice by a diffusion routine were also modified in DNDC-Rice.

In this study, we used the DNDC-Rice model to simulate a soybean system with rye cover crop management and to improve the simulation results by modifying the source codes.

2.2. Modification and Initialization of the Model

At first, the maximum tillage depth was changed—the maximum tillage depth in DNDC-Rice was 20 cm in depth, and it was changed to 30 cm same as field practice. The deepest tilled layer number was also modified. In the DNDC, the deepest tilled layer was set to be 3 when it was less than 3, but it was modified to be 1 when it was less than 1. During the validation, it was found that DNDC-Rice simulated soil C decomposition too fast, and tillage strongly affected soil C decomposition. Therefore, the tillage factor was changed from the default of 1.5 to 1.0. In DNDC-Rice, weeding dates and the degree of

weed growth can be set in three levels (no, moderate, and serious), but we did not set it. Instead, weed biomass input was set as green manure input to reproduce accurate C input. We also modified the temperature limit, T_limit, which was the base degree to calculate thermal degree days (TDD). T_limit for rye was decreased from 10 to 4.4 based on Mirsky et al. [37] to improve the growth. After validating SOC, crop growth, and CO_2 emissions, we examined N_2O and NO emissions but found a serious deviation between simulated and observed values. Through stepwise testing, we modified the emission factors for N_2O and NO from 0.015 to 0.00015 and from 0.0025 to 0.006, respectively, to improve the simulation results.

2.3. Experiment Site

We used a long-term cover crop experiment data, initiated in 2003, at the farm of the Center for International Field Agriculture Research and Education, Ibaraki University, Japan (36°02′ N 140°12′ E). The site is located in a humid subtropical climate, where the average annual precipitation was 1373 mm and the mean daily temperature was 14.5 °C throughout the experimental period (2003–2021) (Figure 1). According to the World Reference Base for Soil Resources, the soil in this region is classified as a typical Andosol. Further details about the site description and soil parameters can be found in Higashi et al. [38].

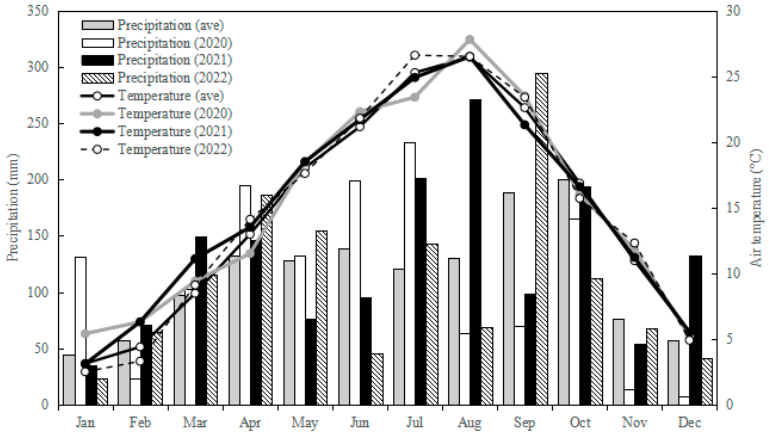

Figure 1. Monthly precipitation and air temperature for 2020, 2021, 2022, and the 2008–2022 average.

2.4. Experiment Design and Field Management

In this experimental field, experiments have been concurrently conducted, employing a range of tillage methods and fertilization management practices. In the present study, the field data were collected from the sub-plot that adopted moldboard plowing without fertilization. The field experiment in this study employed a completely randomized design with four replications, and cover crop management [fallow (FA) vs. rye (RY)] served as the independent variable. Each experimental plot used in this study measured 18 m^2. The main crop in the field experiment was upland rice from 2003 to 2007, after which it was replaced with soybean in 2008. In this study, two cover crop management practices were compared within the soybean system, with four replications for each treatment. The field was plowed twice annually (summer and autumn) to a 30 cm depth using conventional moldboard plowing. Soybean (cv. Sachiyuta) was planted between July and November at a seeding density of 60 kg ha^{-1}. During the cover crop season (November to June), rye (cv. Ryokusei) was sown in the RY plots at a seeding rate of 100 kg ha^{-1}, whereas the FA plots received no artificial intervention, allowing weeds to grow naturally (Table 1). At the termination of the cover crop season, the rye in RY plots and the weeds in FA plots were mowed and returned to the field as green manure. Weed biomass was considered as green manure input exclusively when it occurred within the cover cropping period.

Further details on tillage, crops, and management practices are provided by Table S1 and Gong et al., Higashi et al., and Huang et al. [38–40].

Table 1. Field management schedule for the 2020 and 2021 cropping years. Dates are described as Year/Month/Day.

Management	2020	2021
Summer tillage	2020/6/8	2021/6/14
Soybean sowing	2020/6/30	2021/7/20
Soybean harvest	2020/11/5	2021/11/2
Autumn tillage	2020/11/6	2021/11/3
Cover crop sowing	2020/11/9	2021/11/3
Cover crop harvesting	2021/6/8	2022/5/30

2.5. Soil and Crop Measurement

Soybean samples were collected from the center of each plot using a 0.6 m^2 quadrat on the day of harvest. Biomass was determined by weighing the oven-dried (65 °C for 72 h) samples. The oven-dried samples were then threshed, and the grains were weighed for yield analysis. Aboveground biomass from both rye cover crops in RY plots and natural weeds in FA plots was collected prior to summer tillage using a 0.25 m^2 quadrat. These plant materials were oven-dried (65 °C for 72 h) to a constant mass and weighed to determine dry biomass.

A singular soil core sample was taken from each plot at a depth of 30 cm in October each year for the measurement of SOC. The samples were dried (105 °C for 72 h), ground (2 mm mesh sieve), and analyzed for SOC content using a C/N analyzer (JM3000, J-SCIENCE LAB, Kyoto, Japan). SOC stock was subsequently determined based on SOC content, depth, and soil bulk density using the soil mass equivalent method [41]. Soil temperature at a depth of 0–5 cm was continuously monitored from 2020 to 2021 using soil temperature sensors (TEROS 12, METER Group, Pullman, WA, USA). All soil temperature sensors were installed at the center of experimental plots. Soil volumetric water content was measured during each gas sample collection to determine the water-filled pore space (WFPS) at a depth of 5 cm. More details regarding the measurement and calculation processes of the soybean and soil samples are provided by Gong et al., Higashi et al., and Huang et al. [38–40].

2.6. Greenhouse Gas Measurement

The emissions of N_2O and CO_2 were monitored from June 2020 to May 2022. Weekly gas samples were collected using the static closed chamber method and analyzed with a gas chromatograph (N_2O: GC-ECD, Shimadzu, Kyoto, Japan; CO_2: GC-2014, Shimadzu, Kyoto, Japan) to quantify the concentrations of N_2O and CO_2. Daily fluxes were determined using a concentration–time linear function, while cumulative emissions were calculated through linear interpolation. Further details on the collection, measurement, and calculation of gas samples are shown in Huang et al. and Ratih et al. [40,42].

The net global warming potential (GWP) in agricultural systems consists of greenhouse gas emissions and variation in SOC stock (ΔSOC). The calculation of the net GWP for the period 2020–2021 is as follows:

$$GWP_{2020/2021}\left(CO_2\ equivalent\ \text{kg ha}^{-1}\ \text{year}^{-1}\right) = 265 \times cumulative\ N_2O\ emission_{2020/2021} \quad (1)$$

$$\Delta SOC\ \left(CO_2\ equivalent\ \text{kg ha}^{-1}\ \text{year}^{-1}\right) = \frac{SOC\ stock_{2021} - SOC\ stcok_{2019}}{2} \times \frac{44}{12} \quad (2)$$

$$Net\ GWP_{2020-2021}\ \left(CO_2\ equivalent\ \text{kg ha}^{-1}\ \text{year}^{-1}\right) = \frac{GWP_{2020} + GWP_{2021}}{2} - \Delta SOC \quad (3)$$

where 265 represents the GWP indicator for N_2O conversion to CO_2 over a 100-year period [43]; 44/12 denotes the conversion factor for converting C to CO_2.

2.7. Statistical Analysis

An independent samples *t*-test was performed using SPSS (Version 22.0, IBM, Armonk, NY, USA) to assess the statistical differences between observed and simulated values, with the significance level set at $p = 0.05$. The simulated results, including daily soil temperature, daily water-filled pore space (WFPS), daily N_2O flux, daily CO_2 flux, SOC stock, soybean biomass, and soybean yield, were assessed using the root mean square error (RMSE) calculated as follows:

$$\mathrm{RMSE} = \sqrt{\frac{\sum(\alpha_i - \beta_i)^2}{N}} \quad (4)$$

where α_i and β_i denote the simulated and observed values of parameter i; and N denotes the number of samples. The normalized RMSE (nRMSE) was also used in this study to evaluate the accuracy of the model simulations and was calculated as follows:

$$\mathrm{nRMSE}\ (\%) = \frac{\mathrm{RMSE}}{\overline{\beta}} \times 100 \quad (5)$$

where $\overline{\beta}$ is the average of the observed values.

3. Results

3.1. Soil Temperature and Water-Filled Pore Space

The DNDC-Rice model effectively estimated the daily soil temperature at a depth of 0–5 cm for both the FA and RY systems during the experimental period, with minimal difference between observed and simulated results (Figure 2). The nRMSE of daily soil temperature in the FA system was 10.7%, while in the RY system it was 11.4% (Table 2). The mean simulated soil temperature was marginally higher than the mean observed temperature, with an increase of 2.1% in FA and 1.6% in RY, while these differences were not significant ($p > 0.05$) and remained within acceptable ranges. Overall, the model accurately captured the seasonal fluctuations in soil temperature throughout the year. However, it consistently tended to overestimate soil temperature during the winter months. Field observations across different systems revealed that the mean daily soil temperature in the RY system was slightly higher (1.7%) than in the FA system, although the difference was not significant ($p > 0.05$). Similarly, the model replicated this difference, showing a 1.2% higher ($p > 0.05$) simulated value for the RY system compared to the FA system.

Table 2. Observed and simulated mean soil temperature, water-filled pore space (WFPS), daily N_2O emission, and daily CO_2 emission during the 2020 and 2021 cropping years. FA, fallow; RY, rye; SD, standard deviation; nRMSE, normalized root mean square error.

Variables	Units	Treatment	*n*	Observed Value		Simulated Value		nRMSE (%)
				Mean	SD	Mean	SD	
Soil temperature	°C	FA	678	14.98	0.34	15.29	0.31	10.69
		RY	682	15.24	0.34	15.48	0.31	11.39
WFPS	%	FA	63	32.15	1.39	30.17	0.98	42.67
		RY	63	33.37	1.18	32.56	1.13	41.90
Daily N_2O emission	kg N ha^{-1}	FA	62	1.28	0.17	0.91	0.06	105.16
		RY	63	1.69	0.21	1.63	0.13	94.93
Daily CO_2 emission	kg C ha^{-1}	FA	61	9.07	0.77	10.07	0.99	60.16
		RY	61	14.55	1.26	25.77	1.90	101.31

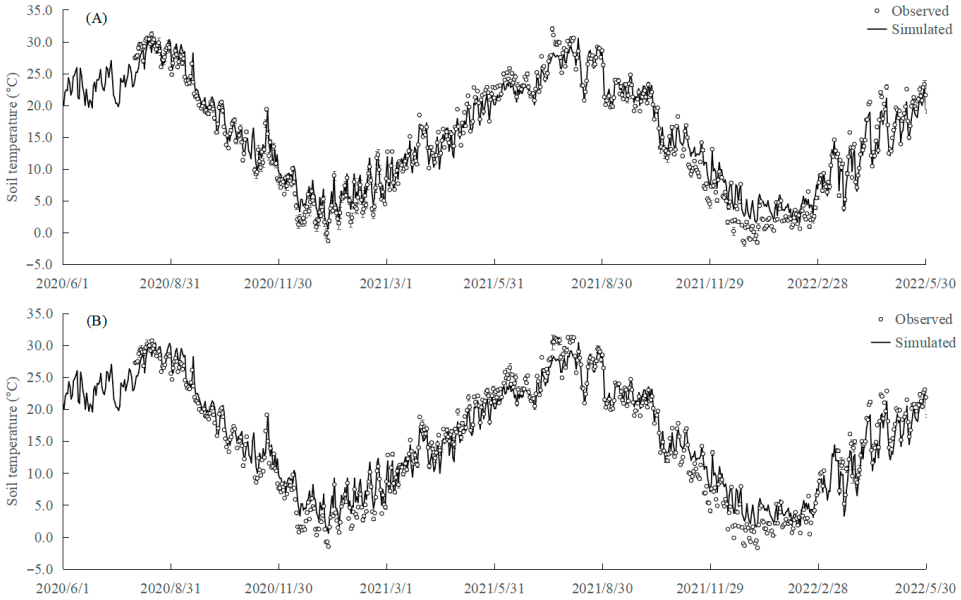

Figure 2. Comparisons between observed and simulated daily soil temperature under fallow (**A**) and rye (**B**) systems during the 2020 and 2021 cropping years.

The DNDC-Rice model successfully simulated the trend of daily WFPS (0–5 cm), although the simulated values were underestimated compared with observed WFPS on average (Figure 3). In the FA system, the mean simulated WFPS was marginally lower (6.2%) than the mean observed value ($p > 0.05$), while in the RY system, it showed a slight reduction by 2.5% ($p > 0.05$) compared to the mean observed WFPS (Table 2). For all cropping systems, the model overestimated the daily WFPS during the winter–spring season but underestimated it during the summer–autumn season. In this study, the nRMSE of WFPS in the FA system was 42.7%, while in the RY system it was 41.9%. The observed mean daily WFPS in the FA system was significantly lower by 3.7% ($p < 0.05$) compared to the RY system, and the model also captured this trend, with the simulated value for the FA system being significantly lower by 7.3% ($p < 0.05$) than that for the RY system.

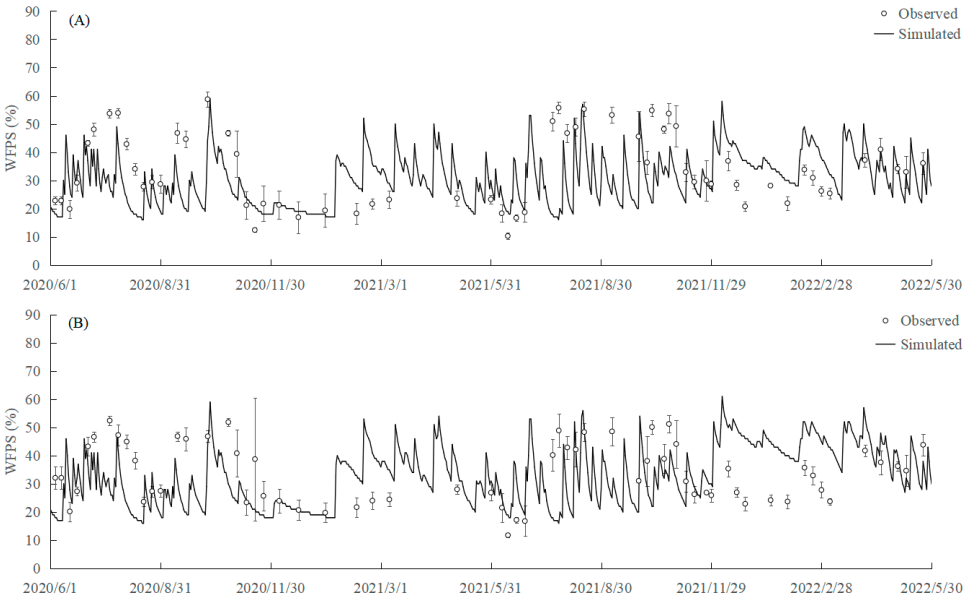

Figure 3. Observed and simulated daily water-filled pore space (WFPS) under fallow (**A**) and rye (**B**) systems during the 2020 and 2021 cropping years.

3.2. Crop Productivity

In order to validate the model's performance on simulating crop productivity, we calculated the average biomass and yield of soybean from 2008 to 2021 compared with simulated values (Table 3). The DNDC-Rice model generally simulated soybean yields accurately in both the FA and RY systems, despite a slight overestimation of the mean simulated values. In the FA system, the model slightly overestimated the mean soybean yield by 3.4% ($p > 0.05$), with an nRMSE of 17.4%. Similarly, in the RY system, the average simulated soybean yield was marginally higher (12.0%) compared to the observed value ($p > 0.05$), with an nRMSE of 17.2%. On the other hand, the DNDC-Rice model overestimated the soybean biomass for both cropping systems. Specifically, the simulated soybean biomass for FA was 15.1% higher than the observed value, whereas for RY it was 18.4% higher. The nRMSE for soybean biomass was 25.5% for FA and 23.5% for RY.

Table 3. Observed and simulated mean soil organic carbon (SOC) stock, soybean biomass, and soybean yield from 2008 to 2021. FA, fallow; RY, rye; SD, standard deviation; nRMSE, normalized root mean square error.

Variables	Units	Treatment	*n*	Observed Value		Simulated Value		nRMSE (%)
				Mean	SD	Mean	SD	
Soybean biomass	Mg C ha^{-1}	FA	13	3.23	0.23	3.72	0.16	25.52
		RY	13	3.13	0.18	3.70	0.16	23.52
Soybean yield	Mg C ha^{-1}	FA	13	1.35	0.11	1.39	0.06	17.44
		RY	13	1.24	0.10	1.38	0.06	17.21
SOC stock	Mg C ha^{-1}	FA	13	80.41	0.88	78.76	0.05	5.38
		RY	13	88.48	1.38	90.43	1.34	4.95

Based on field observations, RY tended to reduce the biomass and yield of soybean, resulting in marginal decreases of 3.2% in mean biomass and 8.8% in mean yield compared to FA, although these differences were not significant ($p > 0.05$). Additionally, the difference in simulated biomass and yield between FA and RY was minimal, with FA showing only a 0.5% increase ($p > 0.05$).

3.3. Soil Organic Carbon and Carbon Dioxide Emission

In the present study, the DNDC-Rice model effectively simulated the variation in SOC stock from 2008 to 2021 (Figure 4 and Table 3). In the FA system, the observed and simulated average SOC stocks were 80.4 Mg C ha^{-1} and 78.8 Mg C ha^{-1}, with an nRMSE of 5.4%. In the RY system, the nRMSE for average SOC stock was 5.0%, with the simulated value (90.4 Mg C ha^{-1}) being 2.2% higher ($p > 0.05$) than the observed value (88.5 Mg C ha^{-1}). Additionally, both the observed and simulated SOC stocks in RY were significantly higher ($p < 0.05$) than those in FA, with increases of 10.0% and 14.8%, respectively.

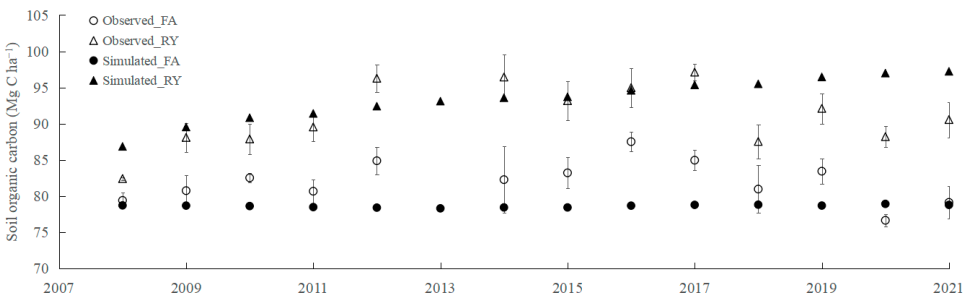

Figure 4. Observed and simulated SOC stock under the fallow (FA) and rye (RY) systems from 2008 to 2021.

During field observations, although surface vegetation within the chamber area was carefully removed, the observed CO_2 emission typically incorporated root respiration due to potential root extension from adjacent areas. To reconcile this observational limitation, the simulated CO_2 emissions in this study also incorporated both soil respiration and root respiration. The DNDC-Rice model reasonably simulated the trend of daily CO_2 emissions across all cropping systems, although it tended to overestimate the actual daily value (Figure 5). The mean simulated daily CO_2 emissions for the FA system were slightly higher by 11.1% than the observed value ($p > 0.05$), with an nRMSE of 60.2%. In the RY system, the model significantly overestimated the mean daily CO_2 by 77.1% ($p < 0.05$), resulting in an nRMSE of 101.3% (Table 2). Additionally, the simulated daily CO_2 flux increased rapidly following each tillage operation. CO_2 flux also exhibited strong seasonal variability, potentially attributable in part to temperature and precipitation anomalies.

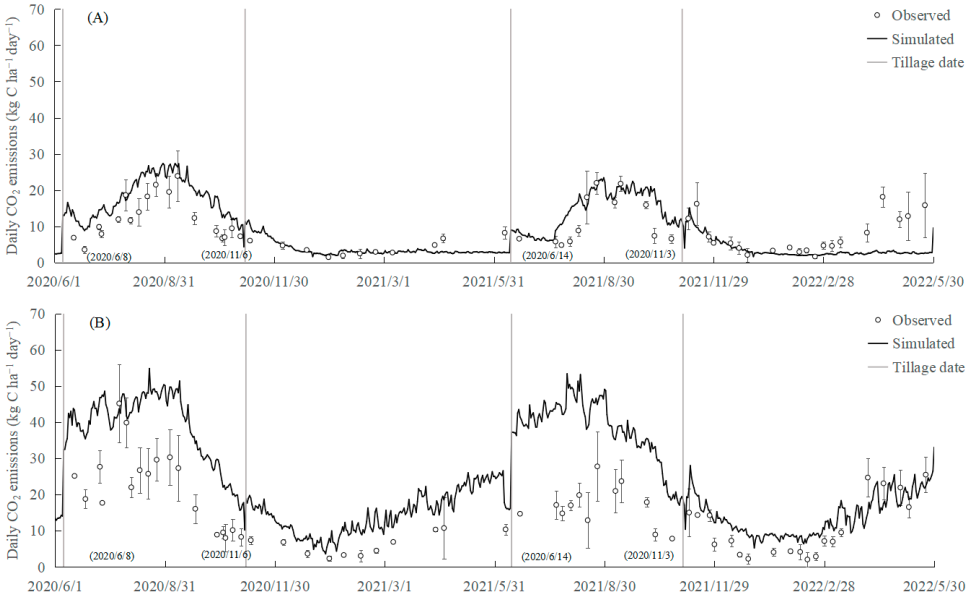

Figure 5. Observed and simulated daily CO_2 emission under the fallow (**A**) and rye (**B**) systems during the 2020 and 2021 cropping years. The gray vertical line, perpendicular to the x-axis, indicates the date of tillage implementation.

Regarding cumulative CO_2 emissions, the model's performance exhibited seasonal variation in the FA system (Table 4). Specifically, during the soybean season, the model overestimated cumulative CO_2 emissions by 42.4% in 2020 and 27.3% in 2021. However, during the cover crop season, the model underestimated cumulative CO_2 emissions, with reductions of 21.3% in 2020 and 53.0% in 2021. In contrast, for the RY system, the model consistently overestimated cumulative CO_2 emissions across all seasons, resulting in an average overestimation of 75.5%. Field observations revealed that the FA system exhibited lower daily CO_2 emissions and total cumulative CO_2 emissions, with reductions of 38% and 34.2%, respectively, compared to the RY system. The model also captured this trend, amplifying the difference, with daily CO_2 emissions and total cumulative CO_2 emissions in the FA system being 60.9% and 62.0% lower, respectively, than those in the RY system.

Table 4. Observed and simulated cumulative CO_2 emissions in each crop season under different cropping systems from 2020 to 2021. FA, fallow; RY, rye.

Variable	Treatment	Observed	Simulated
		kg C ha^{-1}	
2020 Soybean season	FA	1701.37	2422.93
	RY	2869.44	4979.66
2020 Cover crop season	FA	951.51	748.77
	RY	1485.84	3133.97
2021 Soybean season	FA	1421.41	1809.51
	RY	1841.09	3999.32
2021 Cover crop season	FA	1554.02	730.55
	RY	2360.57	2905.00
Total cumulation	FA	5628.32	5711.76
	RY	8556.94	15,017.95

3.4. Soil Nitrous Oxide Emission

In both the FA and RY systems, the DNDC-Rice model effectively captured the seasonal variation trends of daily N_2O emissions throughout the experimental period (Figure 6). However, the model exhibited a poor fit of daily N_2O emission between the simulated and observed values, with a high nRMSE value (105.2% in FA and 94.9% in RY) (Table 2). Compared to the mean observed daily N_2O emission, the simulated value was significantly lower by 28.9% ($p < 0.05$) in the FA system, whereas in the RY system, the reduction was modest (3.5%) and not statistically significant ($p > 0.05$). The model consistently underestimated the cumulative N_2O emissions for the FA system across all crop seasons (Table 5). In the case of the MP system, the cumulative N_2O emissions were underestimated during the soybean season, but overestimated during the cover crop season. Overall, the simulated total N_2O emissions were 25.6% lower than the observed values for the FA system and 5.1% lower for the RY system. Moreover, both the simulated and observed values indicated that the daily N_2O flux and total N_2O emissions under the FA system were lower than those under the RY system, with reductions ranging from 24.3% to 62.0%.

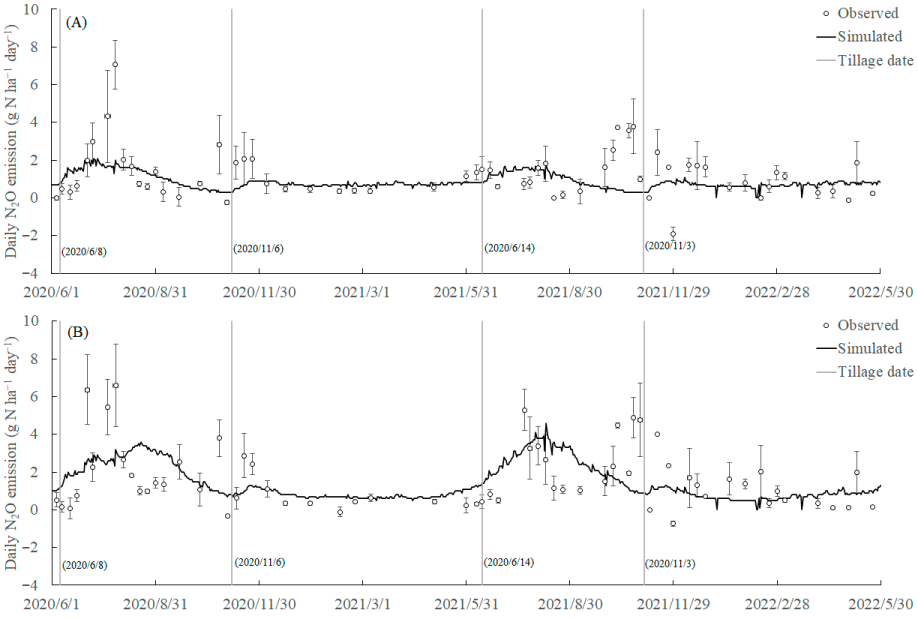

Figure 6. Observed and simulated daily N_2O emissions under the fallow (**A**) and rye (**B**) systems during the 2020 and 2021 cropping years. The gray vertical line, perpendicular to the x-axis, indicates the date of tillage implementation.

Table 5. Observed and simulated cumulative N_2O emissions in each crop season under different cropping systems from 2020 to 2021. FA, fallow; RY, rye.

Variable	Treatment	Observed	Simulated
		kg N ha^{-1}	
2020 Soybean season	FA	231.73	142.80
	RY	335.18	300.30
2020 Cover crop season	FA	150.08	152.20
	RY	126.26	166.90
2021 Soybean season	FA	165.64	92.60
	RY	255.25	267.30
2021 Cover crop season	FA	164.90	142.70
	RY	224.70	158.70
Total cumulation	FA	712.36	530.30
	RY	941.38	893.20

3.5. Global Warming Potential

The net GWP of different cropping systems was assessed and analyzed based on the GWP of N_2O and net CO_2 retention for the period from 2020 to 2021 (Table 6). The simulated N_2O GWP for FA and RY were 20.6% and 2.3% lower, respectively, compared to the field observation. Moreover, RY exhibited a higher N_2O GWP than FA, with observed values showing a 35.9% increase and simulated values a 67.2% increase. For net CO_2 retention, the observed values for FA and RY were −7895.25 and −2833.60 kg CO_2 eq ha^{-1} year^{-1}, whereas the simulated values were 168.82 and 901.60 kg CO_2 eq ha^{-1} year^{-1}. Based on field observation, the net GWP for FA and RY were 8057.58 and 3054.14 kg CO_2 eq ha^{-1} year^{-1}. However, the model simulated minus net GWP values for both FA (−39.96 kg CO_2 eq ha^{-1} year^{-1}) and RY (−686.07 kg CO_2 eq ha^{-1} year^{-1}).

Table 6. Observed and simulated global warming potential (GWP) under different cropping systems during the 2020 and 2021 cropping years. FA, fallow; RY, rye; ΔSOC, change in soil organic carbon stock.

Variable	Treatment	Observed	Simulated
		kg C ha^{-1} year^{-1}	
N_2O GWP	FA	162.33	128.86
	RY	220.53	215.52
ΔSOC	FA	−7895.25	168.82
	RY	−2833.60	901.60
Net GWP	FA	8057.58	−39.96
	RY	3054.14	−686.07

4. Discussion

4.1. Simulation of Soil Temperature, Water-Filled Pore Space, and Crop Growth

Soil temperature and WFPS are vital factors influencing crop growth [44,45]. Simultaneously, those significantly affect N_2O emissions and the decomposition or sequestration of SOC [46,47]. Thus, accurate estimation of soil temperature and WFPS by the DNDC-Rice model is a critical prerequisite for reliably simulating N_2O emissions and SOC stock dynamics. In some versions of the DNDC model, soil surface temperature is assumed to be equal to the daily average air temperature, as the soil temperature profile is calculated based on a heat flux model [22,36]. In contrast, DNDC-Rice integrates a micrometeorological model, enhancing the accuracy of soil temperature profile estimation [29]. Our study findings indicated that DNDC-Rice effectively simulated the soil temperature (0–5 cm) in

both the FA and RY systems, achieving an nRMSE below 12%, which is comparable to or better than results reported in previous studies for upland cropping systems [48,49]. In our study, the simulated WFPS successfully captured the temporal trends of the observed WFPS, consistent with previous findings [49,50]. However, discrepancies were noted in the dynamic values between the observed and simulated WFPS. The observed WFPS was measured manually on gas sampling days, making it susceptible to human error and limited by discontinuous observation periods. The non-continuous observation may have overlooked critical rainfall or drought events, potentially missing the peaks and troughs in WFPS dynamics. Unlike the observed WFPS, which represents point measurements, the simulated WFPS is continuous, calculated at daily time steps, and represents site-averaged values [51,52]. Therefore, owing to the influence of soil heterogeneity, the simulated WFPS values may not align with the observed values. Additionally, a previous study reported that the DNDC-Rice model overestimated water loss through evapotranspiration [53], resulting in an underestimation of soil water content, which is consistent with our results.

Several studies conducted in rice systems have reported that DNDC-Rice tends to overestimate rice straw biomass [53,54]. Similarly, our findings showed that the simulated biomass and yield of soybeans were higher than the observed values. The crop growth sub-model of DNDC-Rice integrates a crop C metabolism model, resulting in simulated crop growth being influenced by N availability and C allocation [29]. The DNDC-Rice model incorporates specific growth functions, calibrated for different rice varieties, to simulate rice growth [31], while it still lacks specific growth functions for other dryland crops, such as soybean and rye. In the empirical crop growth sub-model, plant growth and the allocation ratio of absorbed N are calculated based on TDD, while N uptake is regulated by TDD and the availability of soil N. It is well established that soybean is capable of absorbing and transporting substantial amounts of N through biological N fixation, providing N for utilization by all parts of the plant [55], and N fixation is, of course, assumed in DNDC-Rice. The N fixation rate can be set for each crop as a constant in DNDC-Rice. However, it does not vary with environmental factors and crop growth. The N fixation rate of plants varies across growth stages, while it remains fixed at the original setting in DNDC-Rice simulations [55]. This constant parameterization may lead to overestimation or underestimation of N fixation during different growth stages. Additionally, in field conditions, N fixation increases or decreases as rhizobia increase or decrease, but DNDC-Rice does not predict such temporal variability. Due to the absence of an accurate simulation of biological N fixation in soybean, the DNDC-Rice model may inaccurately estimate N uptake, leading to incorrect simulations of soybean biomass and yield. Therefore, it is essential to develop and calibrate the relevant modules to improve the DNDC-Rice model. For instance, applying different N fixation constants for each growth stage to calculate N uptake using a segmented manner.

4.2. Simulation of Greenhouse Gas Emission and Soil Organic Carbon Stock

While the trend of daily CO_2 flux simulated by the DNDC-Rice model was similar to the observed data, both the daily fluxes and cumulative fluxes were overestimated. Due to the physical disturbance of the soil surface, tillage events often produce a temporary burst of soil CO_2 emission [56]. Following tillage, the DNDC-Rice model exhibited an immediate response, rapidly increasing the simulated daily soil CO_2 flux (Figure 5). In the model, daily CO_2 flux is regulated by the tillage factor. To prevent an excessive increase in CO_2 emissions induced by tillage, this study reduced the tillage factor in the model. In contrast, the observed daily CO_2 flux during the same period showed no significant changes, possibly due to the limitations of discontinuous field sampling, which may have failed to capture the emission peaks induced by tillage events. Consequently, for a period following the

tillage event, the simulated daily soil CO_2 emissions were always higher than the observed values. Soil respiration is divided into autotrophic respiration, primarily driven by plant roots, and heterotrophic respiration, which is mainly driven by microorganisms [57]. In this study, the DNDC-Rice model overestimated soybean biomass, which is associated with a well-developed underground root system. Furthermore, the biomass distribution among various organs during crop growth simulation is determined by the ratios of grain, shoot, and root specified in the crop parameter settings of the DNDC-Rice model. An excessively high root allocation ratio may result in an overestimation of the simulated root biomass. This likely led to an overestimation of root autotrophic respiration during the simulation, resulting in an excessively high CO_2 flux. To avoid this situation, crop parameter settings in the model should be adjusted according to the actual proportional distribution among plant organs. Another main source for the soil CO_2 flux is the soil heterotrophic respiration, which is linked to the sequestration and decomposition of SOC [58]. In the field experiment, both autotrophic and heterotrophic respiration of soil occurred throughout the cover crop season (from November to June) in both the FA and RY systems. Compared to natural weeds in the FA system, the cultivation of cover crops within the RY system contributed to a higher root biomass, thereby enhancing soil autotrophic respiration and resulting in higher CO_2 emissions. In this study, the weeding dates and the degree of weed growth were not set in the model. The absence of the weed growth process would cause the poor accuracy of soil autotrophic respiration during the cover crop season in the FA system. As a result, the simulated CO_2 emissions for the cover crop season in the FA system were lower than the observed values, thereby exacerbating the discrepancy in CO_2 emissions estimation between the FA and RY systems in estimation. Therefore, it must be crucial to improve the accuracy of the weed growth process CO_2 emission.

Some studies have documented that cover crops have the potential to enhance SOC stocks [59,60]. The biomass C from cover crop residues supplies nutrients and energy to soil microorganisms, a portion of which is subsequently converted into microbial C, thereby contributing to an increase in SOC stocks and enhancing C sequestration [61]. The observed SOC stock in the RY system was higher than that in the FA system, and the DNDC-Rice model reproduced these results, although the discrepancy was amplified. These results demonstrate the DNDC-Rice model's capability to accurately simulate the cover crop-induced SOC enhancement. The amplified difference between the FA and RY systems may also be attributed to the absence of the natural weed growth calculation mentioned above, which prevented the DNDC-Rice model from accurately simulating the contribution of weed biomass to the soil C pool in the FA system. Overall, the simulated variation in SOC stock closely followed the observed trend over the period from 2008 to 2021. However, the model could not reproduce the interannual variability observed in the field. In the DNDC model, SOC is automatically allocated to litter, labile humus (humad), and recalcitrant humus pools in a fixed proportion [36], and this same algorithm is also employed in the DNDC-Rice model. However, whether the proportion set within the model aligns with the observed data remains uncertain, as we did not conduct a C composition analysis of the field soil. We speculate that inconsistent allocation proportion and pathways of SOC may be one of the factors contributing to the discrepancies between the model simulations and field observations [36]. Moreover, during the estimation process, the soil bulk density remained consistently aligned with the initial settings. The use of fixed decomposition pools and static bulk density was the current limitation of the model in long-term SOC stock simulations, leading to inadequate representation of interannual SOC variability. Adopting dynamic parameterizations for both soil bulk density and decomposition pools in improved model algorithms may more accurately reflect interannual dynamics of SOC in agroecosystems. In DNDC-Rice, SOC stock was calculated on a daily time step using

predefined equations. In contrast, observed data were gained through manual sampling and measurement at fixed annual time points, which may introduce considerable sampling errors and increase uncertainty.

In the present study, the DNDC-Rice model effectively reproduced the cover crop-induced divergence in N_2O emissions (FA < RY). The reproduction of elevated N_2O emissions in RY systems likely reflects the model's effective parameterization of cover crop decomposition dynamics, particularly the enhanced denitrification potential from increased biomass C and soil moisture retention. Although the DNDC-Rice model effectively captured the seasonal variation in N_2O fluxes, it significantly underestimated the cumulative fluxes. N_2O emissions from soil are commonly released into the atmosphere in a pulsed manner [62], with peak emissions persisting for no more than a few weeks [63]. Meanwhile, in cropping systems, peak N_2O emission events typically account for 50–90% of the annual emissions [64,65]. However, previous studies have identified limitations in the DNDC-Rice model, which fails to accurately predict the timing and magnitude of high N_2O emission pulses [53]. Our findings showed that the simulated daily N_2O fluxes were lower than the observed values during peak N_2O emission events, leading to an underestimation of cumulative N_2O fluxes. Additionally, we observed that the periods of underestimation in daily N_2O fluxes roughly coincided with those of underestimation in WFPS. WFPS is a key driver in the model's simulation of nitrification and denitrification processes, with a profound impact on the prediction of N_2O emissions [66]. Therefore, the discrepancy between the simulated daily N_2O fluxes and observed values is likely due to the underestimation of WFPS. Moreover, because the WFPS in the model was simulated at a daily timestep [51,52], transient peaks induced by short-term rainfall events were diluted through daily averaging, thereby weakening the simulated N_2O pulse effects. Adopting shorter computational timesteps may improve the accuracy of simulating N_2O pulse intensity. Therefore, improving the accuracy of WFPS simulations, as well as modifying the equations governing soil N dynamics to better simulate N_2O emission pulse events, will be key directions for enhancing the DNDC-Rice model's accuracy in predicting N_2O emissions.

Net GWP is derived from the GWP of N_2O and changes in SOC stock in this study, and the substantial interannual variability in observed SOC values also contributes to unavoidable errors in net GWP calculations. Field observations indicated a reduction in SOC stock during the period from 2019 to 2021. In contrast, the DNDC-Rice model, which fits a time-dependent curve for SOC stock based on long-term observational data (2008–2021), simulated an increase in SOC stock during the 2019–2021 period, contradicting the observed results. This inconsistent SOC variation resulted in a discrepancy between the observed and simulated net GWP values. Given the noticeable interannual variation in the observed SOC stock, comparing the observed and simulated net GWP over longer time intervals would be more reasonable.

While this study focused on validating the DNDC-Rice model using observed data from a specific long-term experimental field, we recognize the importance of assessing the model's sensitivity to key input parameters. Therefore, as part of our future research, we plan to conduct a comprehensive sensitivity analysis to gain more generalized insights into the influence of these parameters.

5. Conclusions

This study conducted a field validation of the DNDC-Rice model using data on crop productivity, soil parameters, and GHG fluxes from a soybean system incorporating two cover crop management practices, to evaluate its simulation performance within the context of an upland cropping system. The model accurately simulated soil temperature. However, it underestimated WFPS and N_2O emissions, while overestimating CO_2 emis-

sions, as well as soybean biomass and yield. Moreover, the DNDC-Rice model could reproduce the differences between RY and FA in terms of crop yield, GHG emissions, and SOC stock, although these differences may be exaggerated or diminished due to discrepancies between the simulated and observed values. These findings suggest that certain sub-models within DNDC-Rice—particularly those governing N cycling and crop growth—require algorithmic refinement to enhance their performance in upland cropping systems. Due to algorithmic limitations, the model failed to accurately simulate the growth of soybean and N_2O emission pulse events. Therefore, the crop growth sub-model for upland systems and the N dynamics equations in the DNDC-Rice model required further refinement. Moreover, future work will incorporate a comprehensive sensitivity analysis to further evaluate the influence of key input parameters. Since DNDC-Rice is widely employed in Asia for GHG assessments, the findings of this study could guide modifications to enhance the model's applicability to rotation and mixed cropping systems under conservation agriculture.

Supplementary Materials: The following supporting information can be downloaded at: https://www.mdpi.com/article/10.3390/agriculture15141525/s1, Table S1: Detailed description of field management approaches involved in various systems in this study.

Author Contributions: Q.H.: conceptualization, investigation, data curation, formal analysis, Methodology, visualization, writing—original draft; N.K.: conceptualization, methodology, software, validation, supervision, writing—review and editing, funding acquisition; M.K.: resources, supervision, writing—review and editing; T.F.: methodology, software, writing—review and editing. All authors have read and agreed to the published version of the manuscript.

Funding: This work was supported by the Cross-ministerial Strategic Innovation Promotion Program (SIP), "Building a Resilient and Nourishing Food Supply Chain Management for a Sustainable Future" (Grant Number JPJ012287; funding agency: Bio-oriented Technology Research Advancement Institution).

Institutional Review Board Statement: Not applicable.

Data Availability Statement: Data are available from the corresponding author upon reasonable request.

Conflicts of Interest: The authors declare no conflicts of interest.

References

1. IPCC. *IPCC Climate Change and Land: An IPCC Special Report. Climate Change and Land: An IPCC Special Report on Climate Change, Desertification, Land Degradation, Sustainable Land Management, Food Security, and Greenhouse Gas Fluxes in Terrestrial Ecosystems*; IPCC: Geneva, Switzerland, 2019; pp. 1–864.
2. Malhi, G.S.; Kaur, M.; Kaushik, P. Impact of Climate Change on Agriculture and Its Mitigation Strategies: A Review. *Sustainability* **2021**, *13*, 1318. [CrossRef]
3. Oertel, C.; Matschullat, J.; Zurba, K.; Zimmermann, F.; Erasmi, S. Greenhouse Gas Emissions from Soils—A Review. *Chem. Der Erde* **2016**, *76*, 327–352. [CrossRef]
4. Adetunji, A.T.; Ncube, B.; Mulidzi, R.; Lewu, F.B. Management Impact and Benefit of Cover Crops on Soil Quality: A Review. *Soil Tillage Res.* **2020**, *204*, 104717. [CrossRef]
5. Chen, L.; Rejesus, R.M.; Aglasan, S.; Hagen, S.C.; Salas, W. The Impact of Cover Crops on Soil Erosion in the US Midwest. *J. Environ. Manag.* **2022**, *324*, 116168. [CrossRef] [PubMed]
6. Dai, W.; Feng, G.; Huang, Y.; Adeli, A.; Jenkins, J.N. Influence of Cover Crops on Soil Aggregate Stability, Size Distribution and Related Factors in a No-till Field. *Soil Tillage Res.* **2024**, *244*, 106197. [CrossRef]
7. Haruna, S.I.; Nkongolo, N.V. Influence of Cover Crop, Tillage, and Crop Rotation Management on Soil Nutrients. *Agriculture* **2020**, *10*, 225. [CrossRef]
8. Scavo, A.; Fontanazza, S.; Restuccia, A.; Pesce, G.R.; Abbate, C.; Mauromicale, G. The Role of Cover Crops in Improving Soil Fertility and Plant Nutritional Status in Temperate Climates. A Review. *Agron. Sustain. Dev.* **2022**, *42*, 93. [CrossRef]
9. Büchi, L.; Wendling, M.; Amossé, C.; Jeangros, B.; Charles, R. Cover Crops to Secure Weed Control Strategies in a Maize Crop with Reduced Tillage. *Field Crops Res.* **2020**, *247*, 107583. [CrossRef]

10. Mennan, H.; Jabran, K.; Zandstra, B.H.; Pala, F. Non-chemical Weed Management in Vegetables by Using Cover Crops: A Review. *Agronomy* **2020**, *10*, 257. [CrossRef]
11. Wulanningtyas, H.S.; Gong, Y.; Li, P.; Sakagami, N.; Nishiwaki, J.; Komatsuzaki, M. A Cover Crop and No-Tillage System for Enhancing Soil Health by Increasing Soil Organic Matter in Soybean Cultivation. *Soil Tillage Res.* **2021**, *205*, 104749. [CrossRef]
12. Behnke, G.D.; Villamil, M.B. Cover Crop Rotations Affect Greenhouse Gas Emissions and Crop Production in Illinois, USA. *Field Crops Res.* **2019**, *241*, 107580. [CrossRef]
13. Preza-Fontes, G.; Christianson, L.E.; Greer, K.; Bhattarai, R.; Pittelkow, C.M. In-Season Split Nitrogen Application and Cover Cropping Effects on Nitrous Oxide Emissions in Rainfed Maize. *Agric. Ecosyst. Environ.* **2022**, *326*, 107813. [CrossRef]
14. Peng, Y.; Rieke, E.L.; Chahal, I.; Norris, C.E.; Janovicek, K.; Mitchell, J.P.; Roozeboom, K.L.; Hayden, Z.D.; Strock, J.S.; Machado, S.; et al. Maximizing Soil Organic Carbon Stocks under Cover Cropping: Insights from Long-Term Agricultural Experiments in North America. *Agric. Ecosyst. Environ.* **2023**, *356*, 108599. [CrossRef]
15. Van Eerd, L.L.; Chahal, I.; Peng, Y.; Awrey, J.C. Influence of Cover Crops at the Four Spheres: A Review of Ecosystem Services, Potential Barriers, and Future Directions for North America. *Sci. Total Environ.* **2023**, *858*, 159990. [CrossRef] [PubMed]
16. Basche, A.D.; Miguez, F.E.; Kaspar, T.C.; Castellano, M.J. Do Cover Crops Increase or Decrease Nitrous Oxide Emissions? A Meta-Analysis. *J. Soil Water Conserv.* **2014**, *69*, 471–482. [CrossRef]
17. Singh, H.; Kandel, T.P.; Gowda, P.H.; Northup, B.K.; Kakani, V.G.; Baath, G.S. Soil N_2O Emissions Following Termination of Grass Pea and Oat Cover Crop Residues with Different Maturity Levels. *J. Plant Nutr. Soil Sci.* **2020**, *183*, 734–744. [CrossRef]
18. Guenet, B.; Gabrielle, B.; Chenu, C.; Arrouays, D.; Balesdent, J.; Bernoux, M.; Bruni, E.; Caliman, J.P.; Cardinael, R.; Chen, S.; et al. Can N_2O Emissions Offset the Benefits from Soil Organic Carbon Storage? *Glob. Chang. Biol.* **2021**, *27*, 237–256. [CrossRef] [PubMed]
19. Lugato, E.; Leip, A.; Jones, A. Mitigation Potential of Soil Carbon Management Overestimated by Neglecting N_2O Emissions. *Nat. Clim. Chang.* **2018**, *8*, 219–223. [CrossRef]
20. Abdalla, M.; Hastings, A.; Cheng, K.; Yue, Q.; Chadwick, D.; Espenberg, M.; Truu, J.; Rees, R.M.; Smith, P. A Critical Review of the Impacts of Cover Crops on Nitrogen Leaching, Net Greenhouse Gas Balance and Crop Productivity. *Glob. Chang. Biol.* **2019**, *25*, 2530–2543. [CrossRef] [PubMed]
21. Priya; Singh, S.P. Assessing and Comparing the Sustainability of Organic and Conventional Wheat Farming in India: An Indicator-Based Approach. *J. Clean. Prod.* **2023**, *423*, 138652. [CrossRef]
22. Zhang, Y.; Niu, H. The Development of the DNDC Plant Growth Sub-Model and the Application of DNDC in Agriculture: A Review. *Agric. Ecosyst. Environ.* **2016**, *230*, 271–282. [CrossRef]
23. Abdalla, M.; Song, X.; Ju, X.; Topp, C.F.E.; Smith, P. Calibration and Validation of the DNDC Model to Estimate Nitrous Oxide Emissions and Crop Productivity for a Summer Maize-Winter Wheat Double Cropping System in Hebei, China. *Environ. Pollut.* **2020**, *262*, 114199. [CrossRef] [PubMed]
24. Foltz, M.E.; Kent, A.D.; Koloutsou-Vakakis, S.; Zilles, J.L. Influence of Rye Cover Cropping on Denitrification Potential and Year-Round Field N_2O Emissions. *Sci. Total Environ.* **2021**, *765*, 144295. [CrossRef] [PubMed]
25. Gilhespy, S.L.; Anthony, S.; Cardenas, L.; Chadwick, D.; del Prado, A.; Li, C.; Misselbrook, T.; Rees, R.M.; Salas, W.; Sanz-Cobena, A.; et al. First 20 Years of DNDC (DeNitrification DeComposition): Model Evolution. *Ecol. Model.* **2014**, *292*, 51–62. [CrossRef]
26. Li, C. Modeling Trace Gas Emissions from Agricultural Ecosystems. *Nutr. Cycl. Agroecosyst.* **2000**, *58*, 259–276. [CrossRef]
27. Chang, N.; Chen, D.; Cai, Y.; Li, J.; Zhang, M.; Li, H.; Wang, L. Enhancing Crop Yield and Carbon Sequestration and Greenhouse Gas Emission Mitigation through Different Organic Matter Input in the Bohai Rim Region: An Estimation Based on the DNDC-RF Framework. *Field Crops Res.* **2024**, *319*, 109624. [CrossRef]
28. Katayanagi, N.; Fumoto, T.; Hayano, M.; Shirato, Y.; Takata, Y.; Leon, A.; Yagi, K. Estimation of Total CH_4 Emission from Japanese Rice Paddies Using a New Estimation Method Based on the DNDC-Rice Simulation Model. *Sci. Total Environ.* **2017**, *601–602*, 346–355. [CrossRef] [PubMed]
29. Fumoto, T.; Kobayashi, K.; Li, C.; Yagi, K.; Hasegawa, T. Revising a Process-Based Biogeochemistry Model (DNDC) to Simulate Methane Emission from Rice Paddy Fields under Various Residue Management and Fertilizer Regimes. *Glob. Chang. Biol.* **2008**, *14*, 382–402. [CrossRef]
30. Fumoto, T.; Yanagihara, T.; Saito, T.; Yagi, K. Assessment of the Methane Mitigation Potentials of Alternative Water Regimes in Rice Fields Using a Process-Based Biogeochemistry Model. *Glob. Chang. Biol.* **2010**, *16*, 1847–1859. [CrossRef]
31. Oo, A.Z.; Sudo, S.; Fumoto, T.; Inubushi, K.; Ono, K.; Yamamoto, A.; Bellingrath-Kimura, S.D.; Win, K.T.; Umamageswari, C.; Bama, K.S.; et al. Field Validation of the Dndc-Rice Model for Methane and Nitrous Oxide Emissions from Double-Cropping Paddy Rice under Different Irrigation Practices in Tamil Nadu, India. *Agriculture* **2020**, *10*, 355. [CrossRef]
32. Minamikawa, K.; Fumoto, T.; Iizumi, T.; Cha-un, N.; Pimple, U.; Nishimori, M.; Ishigooka, Y.; Kuwagata, T. Prediction of Future Methane Emission from Irrigated Rice Paddies in Central Thailand under Different Water Management Practices. *Sci. Total Environ.* **2016**, *566–567*, 641–651. [CrossRef] [PubMed]

33. He, D.C.; Ma, Y.L.; Li, Z.Z.; Zhong, C.S.; Cheng, Z.B.; Zhan, J. Crop Rotation Enhances Agricultural Sustainability: From an Empirical Evaluation of Eco-Economic Benefits in Rice Production. *Agriculture* **2021**, *11*, 91. [CrossRef]
34. Minamikawa, K.; Fumoto, T.; Itoh, M.; Hayano, M.; Sudo, S.; Yagi, K. Potential of Prolonged Midseason Drainage for Reducing Methane Emission from Rice Paddies in Japan: A Long-Term Simulation Using the DNDC-Rice Model. *Biol. Fertil. Soils* **2014**, *50*, 879–889. [CrossRef]
35. Li, C.; Frolking, S.; Harriss, R. Modeling Carbon Biogeochemistry in Agricultural Soils. *Glob. Biogeochem. Cycles* **1994**, *8*, 237–254. [CrossRef]
36. Li, C.; Frolking, S.; Frolking, T.A. A Model of Nitrous Oxide Evolution from Soil Driven by Rainfall Events: 2. Model Applications. *J. Geophys. Res.* **1992**, *97*, 9777–9783. [CrossRef]
37. Mirsky, S.B.; Curran, W.S.; Mortensen, D.A.; Ryan, M.R.; Shumway, D.L. Control of Cereal Rye with a Roller/Crimper as Influenced by Cover Crop Phenology. *Agron. J.* **2009**, *101*, 1589–1596. [CrossRef]
38. Higashi, T.; Yunghui, M.; Komatsuzaki, M.; Miura, S.; Hirata, T.; Araki, H.; Kaneko, N.; Ohta, H. Tillage and Cover Crop Species Affect Soil Organic Carbon in Andosol, Kanto, Japan. *Soil Tillage Res.* **2014**, *138*, 64–72. [CrossRef]
39. Gong, Y.; Li, P.; Sakagami, N.; Komatsuzaki, M. No-Tillage with Rye Cover Crop Can Reduce Net Global Warming Potential and Yield-Scaled Global Warming Potential in the Long-Term Organic Soybean Field. *Soil Tillage Res.* **2021**, *205*, 104747. [CrossRef]
40. Huang, Q.; Gong, Y.; Dewi, R.K.; Li, P.; Wang, X.; Hashimi, R.; Komatsuzaki, M. Enhancing Energy Efficiency and Reducing Carbon Footprint in Organic Soybean Production through No-Tillage and Rye Cover Crop Integration. *J. Clean. Prod.* **2023**, *419*, 138247. [CrossRef]
41. Ellert, B.H.; Bettany, J.R. Calculation of Organic Matter and Nutrients Stored in Soils under Contrasting Management Regimes. *Can. J. Soil Sci.* **1995**, *75*, 529–538. [CrossRef]
42. Dewi, R.K.; Gong, Y.; Huang, Q.; Li, P.; Hashimi, R.; Komatsuzaki, M. Addition of Biochar Decreased Soil Respiration in a Permanent No-till Cover Crop System for Organic Soybean Production. *Soil Tillage Res.* **2024**, *237*, 105977. [CrossRef]
43. IPCC. Part A: Global and Sectoral Aspects. Contribution of Working Group II to the Fifth Assessment. In *IPCC Climate Change 2014: Impacts, Adaptation, and Vulnerability*; IPCC: Geneva, Switzerland, 2014.
44. Onwuka, B. Effects of Soil Temperature on Some Soil Properties and Plant Growth. *Adv. Plants Agric. Res.* **2018**, *8*, 89–93. [CrossRef]
45. Hatfield, J.L.; Sauer, T.J.; Prueger, J.H. Managing Soils to Achieve Greater Water Use Efficiency: A Review. *Agron. J.* **2001**, *93*, 271–280. [CrossRef]
46. Butterbach-Bahl, K.; Baggs, E.M.; Dannenmann, M.; Kiese, R.; Zechmeister-Boltenstern, S. Nitrous Oxide Emissions from Soils: How Well Do We Understand the Processes and Their Controls? *Philos. Trans. R. Soc. B Biol. Sci.* **2013**, *368*, 122. [CrossRef] [PubMed]
47. Xu, X.; Shi, Z.; Li, D.; Rey, A.; Ruan, H.; Craine, J.M.; Liang, J.; Zhou, J.; Luo, Y. Soil Properties Control Decomposition of Soil Organic Carbon: Results from Data-Assimilation Analysis. *Geoderma* **2016**, *262*, 235–242. [CrossRef]
48. Li, Z.; Yang, J.Y.; Drury, C.F.; Yang, X.M.; Reynolds, W.D.; Li, X.; Hu, C. Evaluation of the DNDC Model for Simulating Soil Temperature, Moisture and Respiration from Monoculture and Rotational Corn, Soybean and Winter Wheat in Canada. *Ecol. Model.* **2017**, *360*, 230–243. [CrossRef]
49. Abdalla, M.; Song, X.; Ju, X.; Smith, P. Evaluation of the DNDC Model to Estimate Soil Parameters, Crop Yield and Nitrous Oxide Emissions for Alternative Long-Term Multi-Cropping Systems in the North China Plain. *Agronomy* **2022**, *12*, 109. [CrossRef]
50. Nisar, S.; Benbi, D.K.; Toor, A.S. Energy Budgeting and Carbon Footprints of Three Tillage Systems in Maize-Wheat Sequence of North-Western Indo-Gangetic Plains. *Energy* **2021**, *229*, 120661. [CrossRef]
51. Shen, J.; Treu, R.; Wang, J.; Thorman, R.; Nicholson, F.; Bhogal, A. Modeling Nitrous Oxide Emissions from Three United Kingdom Farms Following Application of Farmyard Manure and Green Compost. *Sci. Total Environ.* **2018**, *637–638*, 1566–1577. [CrossRef] [PubMed]
52. Shen, J.; Treu, R.; Wang, J.; Hao, X.; Thomas, B.W. Modeling Growing Season and Annual Cumulative Nitrous Oxide Emissions and Emission Factors from Organically Fertilized Soils Planted with Barley in Lethbridge, Alberta, Canada. *Agric. Syst.* **2019**, *176*, 102654. [CrossRef]
53. Katayanagi, N.; Furukawa, Y.; Fumoto, T.; Hosen, Y. Validation of the DNDC-Rice Model by Using CH_4 and N_2O Flux Data from Rice Cultivated in Pots under Alternate Wetting and Drying Irrigation Management. *Soil Sci. Plant Nutr.* **2012**, *58*, 360–372. [CrossRef]
54. Katayanagi, N.; Ono, K.; Fumoto, T.; Mano, M.; Miyata, A.; Hayashi, K. Validation of the DNDC-Rice Model to Discover Problems in Evaluating the Nitrogen Balance at a Paddy-Field Scale for Single-Cropping of Rice. *Nutr. Cycl. Agroecosyst.* **2013**, *95*, 255–268. [CrossRef]
55. Ciampitti, I.A.; de Borja Reis, A.F.; Córdova, S.C.; Castellano, M.J.; Archontoulis, S.V.; Correndo, A.A.; Antunes De Almeida, L.F.; Moro Rosso, L.H. Revisiting Biological Nitrogen Fixation Dynamics in Soybeans. *Front. Plant Sci.* **2021**, *12*, 727021. [CrossRef] [PubMed]

56. Jackson, L.E.; Calderon, F.J.; Steenwerth, K.L.; Scow, K.M.; Rolston, D.E. Responses of Soil Microbial Processes and Community Structure to Tillage Events and Implications for Soil Quality. *Geoderma* **2003**, *114*, 305–317. [CrossRef]
57. Kuzyakov, Y.; Larionova, A.A. Root and Rhizomicrobial Respiration: A Review of Approaches to Estimate Respiration by Autotrophic and Heterotrophic Organisms in Soil. *J. Plant Nutr. Soil Sci.* **2005**, *168*, 503–520. [CrossRef]
58. Navarro-Pedreño, J.; Almendro-Candel, M.B.; Zorpas, A.A. The Increase of Soil Organic Matter Reduces Global Warming, Myth or Reality? *Sci* **2021**, *3*, 18. [CrossRef]
59. Poeplau, C.; Don, A. Carbon Sequestration in Agricultural Soils via Cultivation of Cover Crops—A Meta-Analysis. *Agric. Ecosyst. Environ.* **2015**, *200*, 33–41. [CrossRef]
60. Repullo-Ruibérriz de Torres, M.A.; Moreno-García, M.; Ordóñez-Fernández, R.; Rodríguez-Lizana, A.; Rodríguez, B.C.; García-Tejero, I.F.; Zuazo, V.H.D.; Carbonell-Bojollo, R.M. Cover Crop Contributions to Improve the Soil Nitrogen and Carbon Sequestration in Almond Orchards (Sw Spain). *Agronomy* **2021**, *11*, 387. [CrossRef]
61. Mendes, I.C.; Bandick, A.K.; Dick, R.P.; Bottomley, P.J. Microbial Biomass and Activities in Soil Aggregates Affected by Winter Cover Crops. *Soil Sci. Soc. Am. J.* **1999**, *63*, 873–881. [CrossRef]
62. Hastings, A.F.; Wattenbach, M.; Eugster, W.; Li, C.; Buchmann, N.; Smith, P. Uncertainty Propagation in Soil Greenhouse Gas Emission Models: An Experiment Using the DNDC Model and at the Oensingen Cropland Site. *Agric. Ecosyst. Environ.* **2010**, *136*, 97–110. [CrossRef]
63. Bell, M.J.; Jones, E.; Smith, J.; Smith, P.; Yeluripati, J.; Augustin, J.; Juszczak, R.; Olejnik, J.; Sommer, M. Simulation of Soil Nitrogen, Nitrous Oxide Emissions and Mitigation Scenarios at 3 European Cropland Sites Using the ECOSSE Model. *Nutr. Cycl. Agroecosyst.* **2012**, *92*, 161–181. [CrossRef]
64. Abdalla, M.; Hastings, A.; Helmy, M.; Prescher, A.; Osborne, B.; Lanigan, G.; Forristal, D.; Killi, D.; Maratha, P.; Williams, M.; et al. Assessing the Combined Use of Reduced Tillage and Cover Crops for Mitigating Greenhouse Gas Emissions from Arable Ecosystem. *Geoderma* **2014**, *223–225*, 9–20. [CrossRef]
65. Wolf, B.; Zheng, X.; Brüggemann, N.; Chen, W.; Dannenmann, M.; Han, X.; Sutton, M.A.; Wu, H.; Yao, Z.; Butterbach-Bahl, K. Grazing-Induced Reduction of Natural Nitrous Oxide Release from Continental Steppe. *Nature* **2010**, *464*, 881–884. [CrossRef] [PubMed]
66. Li, C.; Zhuang, Y.; Cao, M.; Crill, P.; Dai, Z.; Frolking, S.; Moore, B.; Salas, W.; Song, W.; Wang, X. Comparing a Process-Based Agro-Ecosystem Model to the IPCC Methodology for Developing a National Inventory of N_2O Emissions from Arable Lands in China. *Nutr. Cycl. Agroecosyst.* **2001**, *60*, 159–175. [CrossRef]

Disclaimer/Publisher's Note: The statements, opinions and data contained in all publications are solely those of the individual author(s) and contributor(s) and not of MDPI and/or the editor(s). MDPI and/or the editor(s) disclaim responsibility for any injury to people or property resulting from any ideas, methods, instructions or products referred to in the content.